

Two-dimensional link-segment model of the forelimb of dogs at a walk

Cheri Nielsen, MS, DVM; Susan M. Stover, DVM, PhD; Kurt S. Schulz, DVM, MS; Mont Hubbard, PhD; David A. Hawkins, PhD

Objective—To calculate normative joint angle, intersegmental forces, moment of force, and mechanical power at elbow, antebrachiocondylar, and metacarpophalangeal joints of dogs at a walk.

Animals—6 clinically normal mixed-breed dogs.

Procedure—Kinetic data were collected via a force platform, and kinematic data were collected from forelimbs by use of 3-dimensional videography. Length, location of the center of mass, total mass, and mass moment of inertia about the center of mass were determined for each of 4 segments of the forelimb. Kinematic data and inertial properties were combined with vertical and craniocaudal ground reaction forces to calculate sagittal plane forces and moments across joints of interest throughout stance phase. Mechanical power was calculated as the product of net joint moment and the angular velocity. Joint angles were calculated directly from kinematic data.

Results—All joint intersegmental forces were similar to ground reaction forces, with a decrease in magnitude the more proximal the location of each joint. Flexor moments were observed at metacarpophalangeal and antebrachiocondylar joints, and extensor moments were observed at elbow and shoulder joints, which provided a net extensor support moment for the forelimb. Typical profiles of work existed for each joint.

Conclusions and Clinical Relevance—For clinically normal dogs of a similar size at a walk, inverse dynamic calculation of intersegmental forces, moments of force, and mechanical power for forelimb joints yielded values of consistent patterns and magnitudes. These values may be used for comparison in evaluations of gait in other studies and in treatment of dogs with forelimb musculoskeletal disease. (*Am J Vet Res* 2003;64:609–617)

The application of an inverse dynamics approach to calculate net joint moments from morphometric, positional, and force data is a classic technique in biomechanical gait analysis.¹ An abundance of informa-

tion exists in the human literature regarding the moments applied to, and the power generated by, joints of the lower portion of the limb by the surrounding musculature, beginning with Bresler and Frankel's landmark study in 1950² and continuing through this decade. Application of moment and power data to the clinical setting has made a great impact on the standard of care within the orthopedic and rehabilitation communities regarding evaluation, prognosis, and treatment. Many advances in the knowledge of the mechanisms of specific human orthopedic and gait disorders have come from quantitative gait analysis, and it is common practice to quantify clinical gait deficits in human patients with these techniques.

In the field of veterinary medicine, several studies^{3–8} in dogs or horses have been conducted by use of kinetic force platform data or kinematic motion data over the past decade. However, kinetic data and kinematic data have rarely been combined to produce a thorough dynamic gait analysis. Of the few such published works, 1 study⁴ calculated the moments and power for the equine thoracic limb at a walk⁶ and trot to provide benchmark data for clinical use. Another study⁵ performed a similar analysis of the pelvic limb of dogs at a walk to compare intersegmental forces at the hip joint before and after total hip arthroplasty. In a pair of studies,^{7,8} net joint powers and energies were calculated during the swing phase of the stride in hind limb of walking⁸ and trotting⁷ horses. To our knowledge, no such analyses have been reported for the canine thoracic limb.

Body segment parameters (including length, location of the center of mass, total mass, and mass moment of inertia) of the individual segments are needed in addition to kinetic and kinematic data for inclusion of gravitational and inertial forces in gait analyses. Body segment data have traditionally been collected by direct measurement, which is time-consuming and requires cadaveric specimens. Historically, only a few such studies^{9–17} in humans have been performed (with a total of ≤ 50 cadavers measured, predominantly adult male Caucasians). However, collectively, these published data have frequently been applied in development of mathematic models of the human body and in analysis of human motion.¹⁸

The limited reported data are not sufficient to capture the large individual variation in body segment parameters for people. Clauser¹³ developed regression equations to predict the necessary parameters for an individual from anthropometric measurements easily obtained on living subjects. More recently, individual body segment parameters have been

Received July 8, 2002.

Accepted October 16, 2002.

From the J.D. Wheat Veterinary Orthopedic Research Laboratory, School of Veterinary Medicine (Nielsen, Stover, Schulz), the Department of Mechanical and Aeronautical Engineering (Hubbard), College of Engineering, and the Human Performance Laboratory, Division of Biological Sciences, (Hawkins) University of California, Davis, CA 95616. Dr. Nielsen's current address is the Colorado State University Veterinary Teaching Hospital, Fort Collins, CO 80523.

Supported by grants from the Achievement Rewards for College Scientists Foundation and by an American Association of University Women graduate fellowship.

Address correspondence to Dr. Stover.

determined from living subjects by use of noninvasive techniques such as fluid displacement,¹⁹ stereophotometry,²⁰ ultrasonography,²¹ optoelectronic volumetry,^{22,23} magnetic resonance imaging,^{24,25} and computerized tomography.²⁶⁻²⁹

To our knowledge, no body segment parameter data or regression equations have been published for veterinary patients, and noninvasive techniques are time-consuming and costly. As a result, studies of domestic animals require direct measurement of body segment parameters for each individual. This necessitates a terminal research protocol and makes studies of clinical patients unfeasible.

The primary objective of the study reported here was to determine joint angular position, intersegmental forces, joint moment of force, and mechanical power at the elbow, antebrachiocondylar, and metacarpophalangeal joints of dogs at a walk. A second objective was to present the necessary body segment parameters of the dogs of our study for reference in future studies that use dogs of comparable size. It is expected that our study of the canine forelimb will provide necessary reference data for future quantitative studies of orthopedic disorders.

Materials and Methods

Animals—Six clinically normal adult mixed-breed dogs (mean \pm SD] body mass, 25.3 ± 2.5 kg; 3 males and 3 females) were studied after protocol approval by the University of California, Davis Animal Use and Care Committee. Dogs were used for unrelated, terminal studies between collection of kinetic and kinematic data and measurement of body segment parameters. No musculoskeletal abnormalities were observed during clinical orthopedic examination for all dogs. All dogs were in good body condition and not overtly obese. None of the dogs had a chondrodysplastic phenotype.

Experimental protocol—Kinetic and kinematic data were collected simultaneously from walking dogs. Kinetic data (3 components of force) were collected at 1,000 Hz from a force platform^a mounted flush with the surface of a 15 m walkway by use of data acquisition computers.^{b,c} Kinematic data were collected at 200 Hz from 3 synchronized video cameras^d interfaced to a multiple-frequency video image processor.^e The 3-dimensional (D) positions of reflective joint center markers were quantified over time within a calibrated test space ($32 \times 40 \times 56$ cm) centered over the force platform. Sixteen spherical markers^f of known locations were used to calibrate the test space in the positive quadrant of a right-handed orthogonal coordinate axes system. Kinetic data acquisition was initiated by a manual trigger that was started by the operator prior to the dog contacting the force platform so that no data were lost. Kinematic data acquisition was initiated and synchronized with kinetic data acquisition by a digital trigger.

Reflective markers were secured with cyanoacrylate adhesive to shaved skin overlying the approximate centers of the left shoulder, elbow, antebrachiocondylar, and metacarpophalangeal joints, and over the most proximolateral aspect of the 4th middle phalanx (Fig 1). Each dog was led at a walk in a straight line through the calibrated test space with the objective of maintaining a forward velocity between 0.8 and 1.0 m/s. Forward velocity was controlled by the handler and verified by kinematic analysis of the shoulder marker. Ten valid trials were collected for each dog. A trial was valid when a strike of only the left paw occurred completely on the force platform, all reflective

markers were visible in the test space by at least 2 cameras, and no tension on the lead nor other observed irregularity of straight forward motion was observed. Generally, the markers were visible by all 3 cameras so that the least-squares method could be used in calculating position data, thus increasing the accuracy.

Three of the valid trials from each dog were selected for analysis on the basis of consistency of stance duration, peak force, and contour of the vertical ground reaction force data. Stance duration has been previously shown³⁰ to accurately reflect changes in velocity and ground reaction forces in force platform evaluations in dogs.

Kinetic data—Because motion of the canine forelimb is predominantly in the sagittal plane, only the vertical and craniocaudal components of the ground reaction force data were analyzed. Data collected at 1,000 Hz were reduced to 200 Hz for ease of processing after visually ascertaining that unique features of the data were not lost. Vertical and craniocaudal ground reaction forces were normalized by the dog's body weight and reported as percentage of body weight. Vertical ground reaction force data were used to determine initiation and termination of the stance phase of the left forelimb in the gait cycle. Time data were normalized by duration of the stance phase for each trial and reported in 2% intervals as a percentage of the total stance phase.

Kinematic data—Kinematic data were filtered at acquisition with a fourth-order Butterworth low pass filter, with a

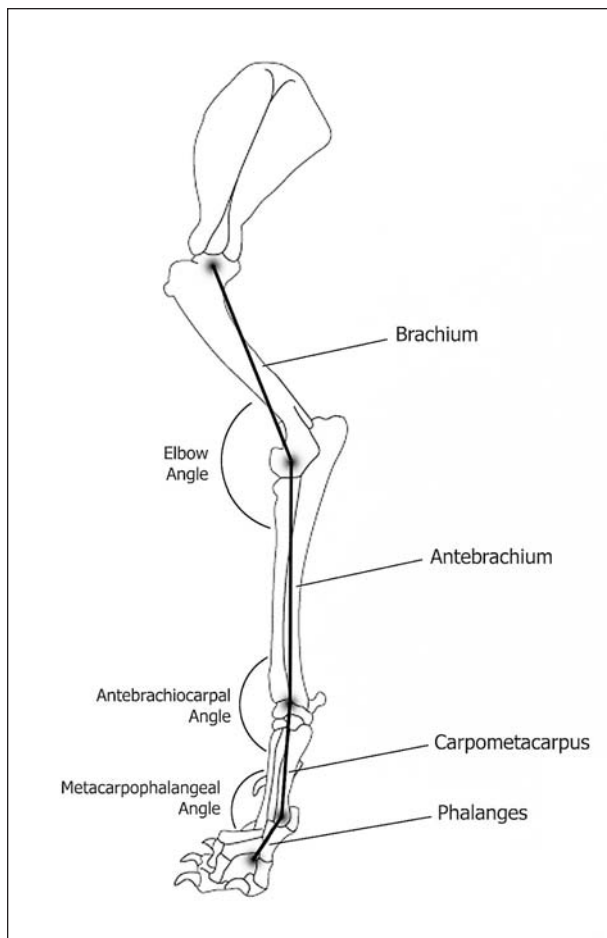


Figure 1—Drawing of the anatomic location of body segments, joint angles, and kinematic markers on the bones of the canine forelimb.

cutoff frequency of 10 Hz, to attenuate noise in the signal. Examination of the 3-D data revealed only small deviations in position from the 2-D plane of forward motion. Therefore, joints were assumed to be acting as pure hinge joints in the sagittal plane. Kinematic data were condensed from 3-D coordinates to 2-D coordinates in the sagittal plane (that plane generally corresponding to the individual's forward motion).

Position data for the joint centers were used to obtain angles between each segment and the horizontal plane over time for the duration of the stance phase. A cubic spline was fit to the angular position versus time data. Angular velocities and accelerations were determined by calculating the first and second derivatives, respectively, of the cubic spline functions.

Body segment parameters—After euthanasia by IV injection of a sodium pentobarbital solution,⁵ the left forelimb was removed from each cadaver. The forelimb segments were isolated by disarticulation of the shoulder, elbow, antebrachiocondylar, and metacarpophalangeal joints. The location of the center of mass was determined for each segment by use of a balance technique.³¹ Limb segment masses and lengths were measured directly.^h Lengths were measured between approximate joint centers corresponding to the skin markers placed for kinematic data acquisition. Mass moments of inertia were determined by use of a pendulum technique.³¹ The limb segment was allowed to swing from a horizontal position around a fixed mediolateral axis that was a known distance from the segment's center of mass. A rotary variable inductance transducerⁱ was used with laboratory acquisition software^j to record the angle of the segment over time at 200 Hz. A cubic spline was fit to the data, and the second time derivative of the spline function was calculated^k to determine the angular acceleration of the segment. The parallel-axis theorem was used to

obtain the mass moment of inertia about the center of mass for each segment in the sagittal plane.

Inverse dynamic method—A 2-D inverse dynamic solution was applied by use of a link-segment model^l to calculate intersegmental reaction forces and moments. Assumptions³¹ inherent to the model were that each body segment has a constant mass, constant length, fixed center of mass, and constant mass moment of inertia about its center of mass throughout the movement, and that all joints act as simple hinge joints.

Positive joint moments³¹ correspond to a net positive joint muscle moment that causes elevation of the body's mass, typically by joint extension. Joint mechanical power was calculated as the product of the net joint moment and the joint angular velocity. The location of the reported joint angles, on the cranial aspect of the limb, was based on clinical convention (Fig 1). In reporting the results as figures, a positive moment represents force by the extensor muscles across the joint. Similarly, a positive mechanical power profile represents net work by the extensor muscles across the corresponding joint.

Results

Body segment parameters—The coefficients of variation for the body segment parameters varied from 3 to 38%. The largest coefficients of variation were observed in the mass moment of inertia (14 to 38%). All other body segment parameters had coefficients of variation < 13% (Table 1).

Temporal variables—Kinematic data for Dog 3 became corrupt so that the position coordinates could not be extracted from the binary file. As the data were unavailable, Dog 3 was excluded completely from the

Table 1—Mean (± SD) body segment parameters of 6 dogs with a mean (± SD) body mass of 25.3 ± 2.5 kg

| Measurements | Segments | | | |
|--|-------------|-----------------|--------------|-------------|
| | Phalangeal | Carpometacarpal | Antebrachial | Brachial |
| Mass (%) [*] | 0.32 ± 0.04 | 0.38 ± 0.04 | 1.26 ± 0.12 | 2.99 ± 0.35 |
| Length (cm) | 5.2 ± 0.5 | 8.4 ± 0.6 | 18.2 ± 0.7 | 17.8 ± 0.5 |
| Center of mass (%) [†] | 50.0 ± 2.8 | 52.9 ± 3.7 | 59.0 ± 2.3 | 53.1 ± 2.7 |
| Mass moment of inertia (kg•cm ²) | 0.8 ± 0.3 | 1.4 ± 0.3 | 14 ± 2.0 | 55 ± 11 |

^{*}Percentage of total body mass. [†]Percentage of total length as measured from the distal end of segment.

Table 2—Mean (± SD) temporal variables, peak ground reaction forces, and peak vertical intersegmental force of 6 dogs with a mean (± SD) body mass of 25.3 ± 2.5 kg

| Measurements | Dogs | | | | | | Overall |
|------------------------|--------------|--------------|--------------|--------------|--------------|--------------|--------------|
| | 1 | 2 | 3 | 4 | 5 | 6 | |
| Temporal variables | — | — | — | — | — | — | — |
| Forward velocity (m/s) | 0.94 ± 0.01 | 0.78 ± 0.10 | 0.96 ± 0.02 | 0.92 ± 0.01 | 0.78 ± 0.02 | 0.84 ± 0.09 | 0.84 ± 0.09 |
| Stance duration (s) | 0.53 ± 0.05 | 0.50 ± 0.06 | 0.47 ± 0.04 | 0.54 ± 0.02 | 0.55 ± 0.04 | 0.55 ± 0.06 | 0.52 ± 0.05 |
| PGRF | — | — | — | — | — | — | — |
| Vertical (% BW) | 53.02 ± 2.29 | 63.82 ± 3.11 | 64.95 ± 0.93 | 63.93 ± 0.56 | 59.83 ± 2.15 | 66.82 ± 1.64 | 62.60 ± 4.53 |
| Craniocaudal (% BW) | 11.99 ± 0.46 | 9.10 ± 1.83 | 13.40 ± 2.77 | 13.99 ± 1.45 | 10.47 ± 0.47 | 10.52 ± 1.69 | 11.55 ± 2.31 |
| PVIF | — | — | — | — | — | — | — |
| MCP joint (% BW) | 52.73 ± 2.29 | 63.27 ± 3.25 | NA | 63.55 ± 0.57 | 59.53 ± 2.15 | 66.49 ± 1.64 | 61.71 ± 4.83 |
| ABC joint (% BW) | 52.35 ± 2.29 | 62.93 ± 3.26 | NA | 63.15 ± 0.56 | 59.20 ± 2.15 | 66.10 ± 1.65 | 61.35 ± 4.81 |
| Elbow joint (% BW) | 51.09 ± 2.29 | 61.66 ± 3.27 | NA | 62.03 ± 0.56 | 57.92 ± 2.15 | 64.81 ± 1.65 | 60.10 ± 4.83 |
| Shoulder joint (% BW) | 47.90 ± 2.29 | 58.78 ± 3.32 | NA | 58.95 ± 0.56 | 55.18 ± 2.17 | 62.12 ± 1.66 | 57.21 ± 4.94 |

PGRF = Peak ground reaction force. PVIF = Peak vertical intersegmental force. MCP = Metacarpophalangeal. ABC = Antebrachiocondylar. BW = Body weight. NA = Not available.

inverse dynamic analysis and the reporting of joint angles. Mean (\pm SD) forward velocity was 0.84 ± 0.09 m/s, and mean total stance duration was 0.53 ± 0.05 second across all 18 trials (Table 2).

Ground reaction and intersegmental forces—Mean peak vertical force was $62.6 \pm 4.5\%$ of body weight, and mean peak craniocaudal force was $11.6 \pm 2.3\%$ of body weight (Table 2, Fig 2). The craniocaudal force curve was nearly symmetric, so that the peak propulsive force was similar to the peak braking force during stance.

Mean peak craniocaudal intersegmental force was

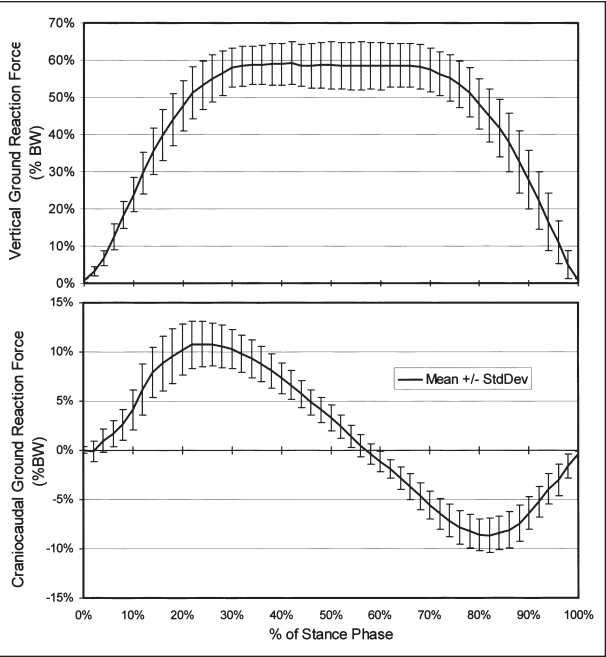


Figure 2—Mean (\pm SD) forelimb ground reaction forces (% body weight [BW]) versus the percentage of stance phase in 6 dogs.

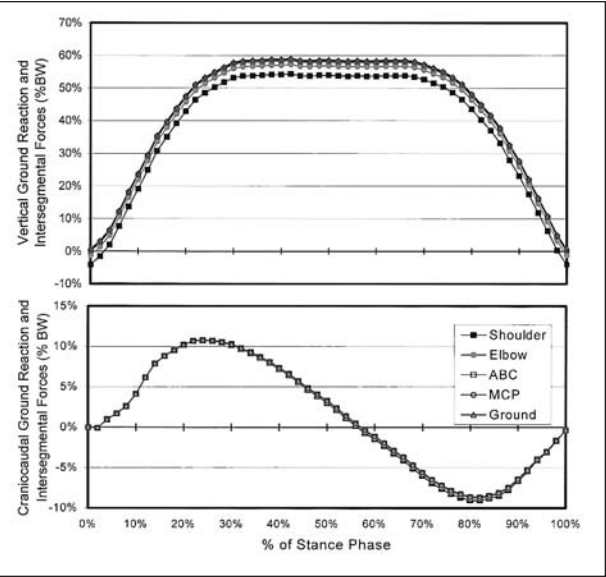


Figure 3—Mean (\pm SD) forelimb ground reaction and intersegmental forces (% BW) versus the percentage of stance phase in 5 dogs. ABC = Antebrachioacarpal. MCP = Metacarpophalangeal.

$11.1 \pm 2.1\%$ of body weight for all intersegmental joints (Fig 3). Mean peak vertical forces of the metacarpophalangeal, antebrachioacarpal, elbow, and shoulder joints were 61.7 ± 4.8 , 61.3 ± 4.8 , 60.0 ± 4.8 , and $57.2 \pm 4.9\%$ of body weight, respectively.

Metacarpophalangeal joint—The metacarpophalangeal joint began stance phase at a mean value of $132.7 \pm 27^\circ$ of extension and fluctuated $< 5^\circ$ on average during the first half of stance (Fig 4). It then flexed slowly and steadily to a mean maximum of $144.8 \pm 40^\circ$ just before lift-off and extended slightly in the final 5% of the stance phase.

A net flexor moment at the metacarpophalangeal joint throughout most of stance phase was observed, with a net extensor moment just before take-off in some trials but only a decreasing flexor moment in others (Fig 4). The power profile of the metacarpophalangeal joint had short phases of positive and negative work against the predominant flexor moment throughout the stance phase, reflecting the small angular displacement of the joint.

Antebrachioacarpal joint—The antebrachioacarpal joint began stance phase at a mean value of $192.4 \pm 25^\circ$ of extension and continued to extend over the first 3-quarters of the stance phase to a mean minimum of $154 \pm 20^\circ$ (Fig 5). It then flexed at a faster rate until lift-off, by which time it had returned approximately to its initial position ($198.3 \pm 27^\circ$).

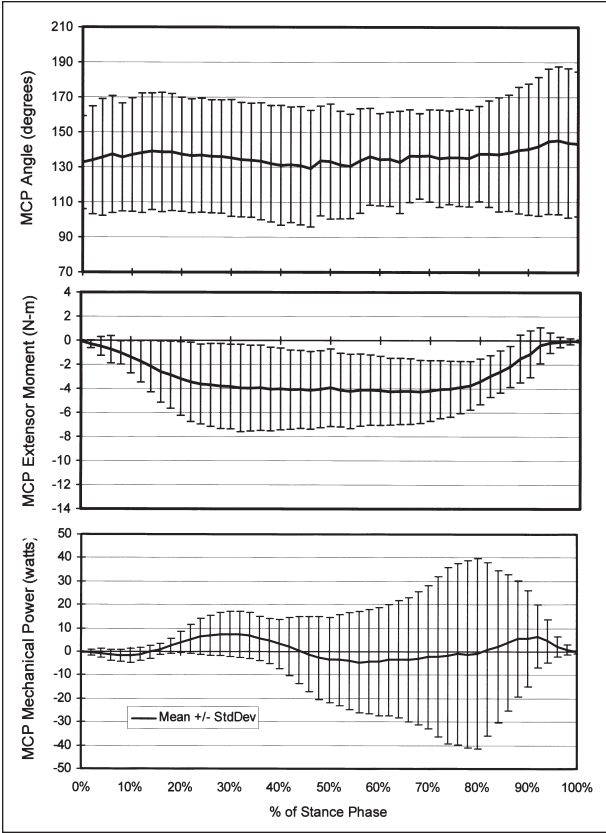


Figure 4—Mean (\pm SD) joint angle, moment of force, and mechanical power at the MCP joint versus the percentage of stance phase in 5 dogs.

A net flexor moment at the antebrachioacarpal joint throughout most of stance phase was observed, with a net extensor moment just before take-off in some trials but only a decreasing flexor moment in others (Fig 5). The power profile of the antebrachioacarpal joint revealed that positive work was performed by the extensor muscles throughout the first 3-quarters of the stance phase, which was coincident with extension of the joint. The power profile became negative in the last quarter of the stance phase, indicating net work by the antebrachioacarpal flexors as the joint flexed to return to its initial position.

Elbow joint—The elbow joint began stance phase at a mean value of $111.7 \pm 12^\circ$ of flexion and immediately extended slightly, then flexed to return to its starting position during weight acceptance in early stance (Fig 6). It then extended steadily throughout stance to a mean maximum of $136.3 \pm 10.4^\circ$ and flexed slightly just before lift-off in terminal stance.

A net extensor moment at the elbow throughout most of the stance phase was observed, with a net flexor moment just before take-off coincident with the change at the elbow from extension to flexion (Fig 6). The power profile of the elbow revealed negative work early in stance, followed by positive work by the extensor muscles of the elbow for most of the stance phase and a brief return to negative work at take-off.

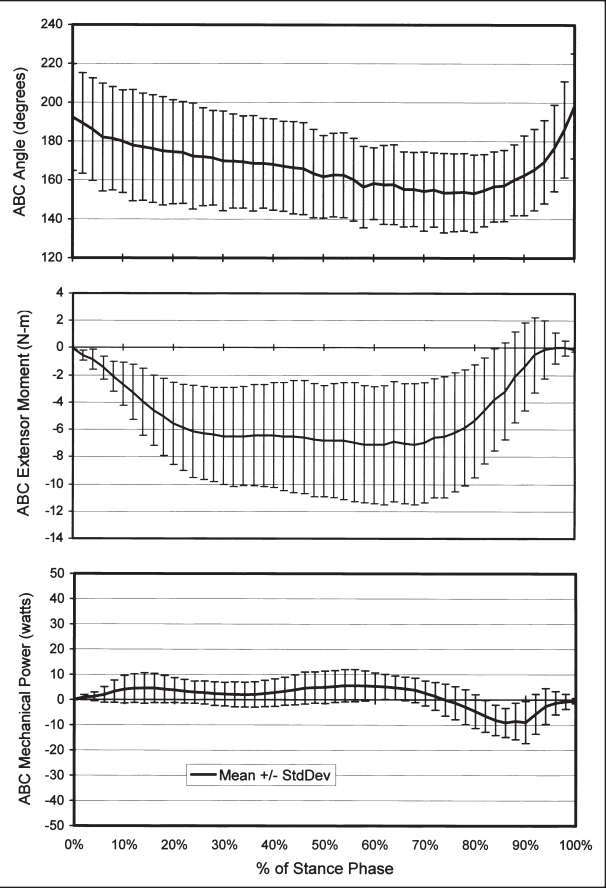


Figure 5—Mean (\pm SD) joint angle, moment of force, and mechanical power at the ABC joint versus the percentage of stance phase in 5 dogs.

Shoulder joint—Angular position and mechanical power of the shoulder joint were not calculated, as no reflective marker was placed over the scapula. Shoulder moment had a net extensor moment throughout most of stance phase (Fig 7).

Net support moment—The sum of the joint moments was calculated across the shoulder, elbow, antebrachioacarpal, and metacarpophalangeal joints. A net extensor moment throughout stance phase for support of the forelimb was observed (Fig 8).

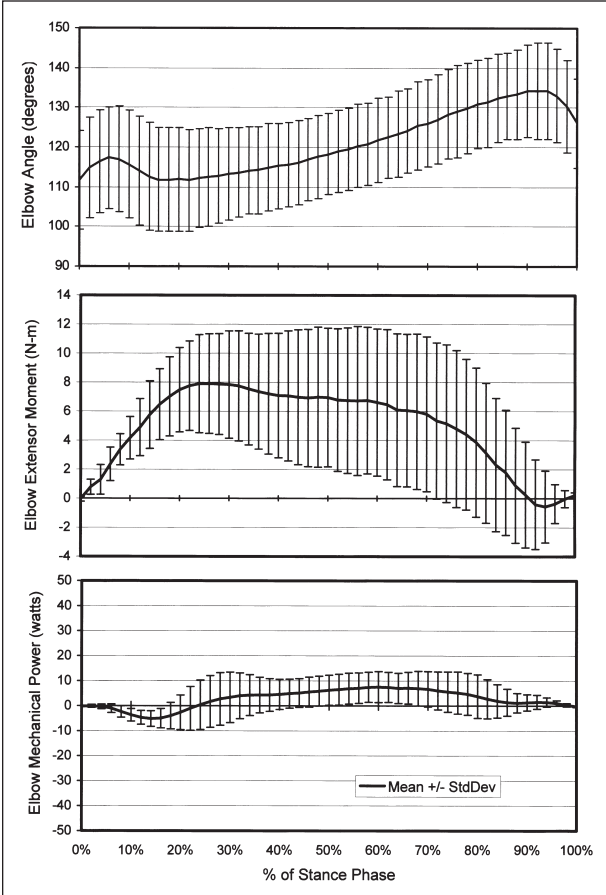


Figure 6—Mean (\pm SD) joint angle, moment of force, and mechanical power at the elbow joint versus the percentage of stance phase in 5 dogs.

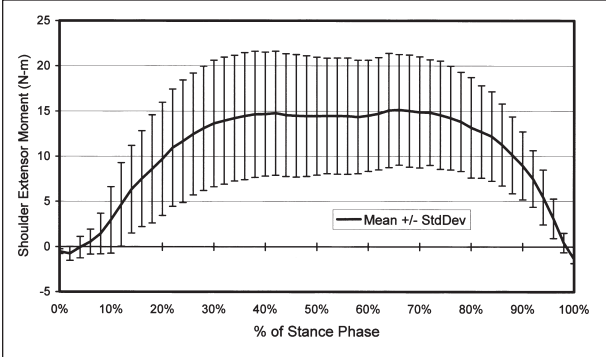


Figure 7—Mean (\pm SD) moment of force at the shoulder joint versus the percentage of stance phase in 5 dogs.

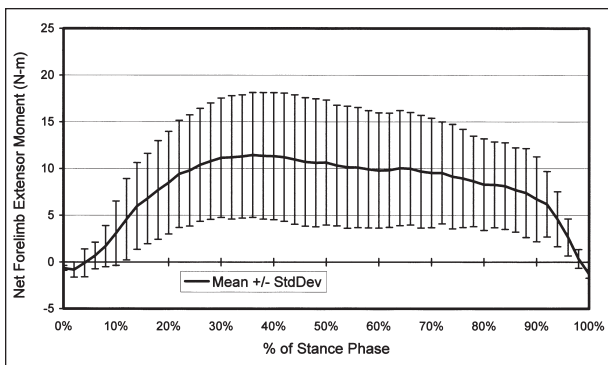


Figure 8—Mean (\pm SD) net forelimb extensor moment versus the percentage of stance phase in 5 dogs.

Discussion

In our study, we evaluated joint angular position, intersegmental forces, joint moment of force, and mechanical power during the stance phase for the canine elbow, antebrachiocondylar, and metacarpophalangeal joints in walking dogs with a normal gait. At a walking gait, intersegmental forces were found to be similar in form to the measured ground reaction forces, with an overall small decrease in magnitude the more proximal the location of each joint. A net flexor moment was observed at the metacarpophalangeal and antebrachiocondylar joints, and a net extensor moment was observed at the elbow and shoulder joints; together, they provide a net extensor support moment for the forelimb throughout stance. Typical profiles of work existed for the elbow, antebrachiocondylar, and metacarpophalangeal joints, although a large SD was found for values of the metacarpophalangeal joint. In our study, angular position at all 3 joints and all body segment parameters of the mixed-breed dogs evaluated were consistent, despite visual differences in conformation.

Data from our study provide a basic characterization of kinematics and physiologic loading of the joint in clinically normal dogs, which can be used in mathematical or mechanical models of motion involving the normally functioning canine forelimb. Our results provide baseline data necessary for objective investigation into alterations of joint loading and motion with elbow disease, as part of the ongoing debate over the pathophysiologic changes and treatment of elbow dysplasia, the major orthopedic disorder of the canine forelimb. Our data may also contribute to the design of surgical implants, such as a successful elbow arthroplasty system for dogs. Additionally, these normative data provide a benchmark against which to compare these variables in dogs with specific lameness as dynamic gait analysis becomes more widely available and applicable to veterinary clinical patients.

Some error is associated with the reduction of 3-D kinematic data to 2-D data. Overall, this transformation process is expected to reduce out-of-plane measurement error inherent in single-camera, 2-D studies, although a difference between the mathematical plane of the coordinates and that of the individual's actual progression may still exist. Assessment of the effect of this transformation indicated differences of $< 2\%$ in segment lengths between those calculated from 3-D

data and 2-D data. These small differences in length will nevertheless affect the accuracy of force, moment, and power data.

Another potential source of error in our study is in the placement of the skin markers over the presumed joint centers. This would contribute to decreased accuracy of kinematic data and in turn would affect the calculated forces, moments, and powers. One study in humans³² calculated variability in joint angles as a result of marker placement by attaching markers to the same individual multiple times and reported a SD in flexion and extension angles of 1.0° each at the ankle and knee joints and 1.7° at the hip joint. The effect of variability in marker placement was not evaluated in our study. This particular source of error has been discussed in other studies in dogs that used kinematic data,^{5,33} but no attempts were made to quantify or compensate for the error.

Movement of the skin markers relative to the skeleton also introduces error. In other veterinary studies,^{34,36} the effect of skin movement during kinematic data collection has been evaluated. Results of a pair of studies^{34,35} in horses, revealed that markers on the skin over the metacarpophalangeal joint displaced approximately 2 mm, and markers placed over the carpal joint moved up to 11 mm relative to indwelling light-emitting diodes throughout the walking gait cycle. However, other joints were not evaluated, and the anatomy of the distal portion of the limb is considerably different between horses and dogs, so it is not clear how to apply these findings to those of our study.

To decrease variability introduced from any 1 of these sources, the lengths of the body segments obtained by direct measurement rather than those extracted from the joint marker positions were used in calculating intersegmental forces, moments, and mechanical power at each joint. The difference between calculated length and measured length varied throughout stance and by body segment. The variation in length as calculated from kinematic data throughout stance within a trial was $< 5\%$ of length for all body segments and trials. The difference between the mean calculated length across trials for a given dog and the measured length was greatest for the brachial segment, with a mean difference in length of 14.0% (range, 11.0 to 16.6%). Mean differences as a percent of length for the antebrachial, carpometacarpal, and phalangeal segments were 1.3 (range, 0.3 to 2.3%), 8.7 (range, 4.5 to 14.8%), and 7% (range, 5.9 to 8.0%), respectively. The brachial segment most likely had the greatest difference as a result of the large amount of skin and musculature overlying the skeleton near the torso at the proximal end of the segment. The variation in this particular segment affects calculation of joint angular position and mechanical power at the elbow joint, the intersegmental forces, and the moment of force at the shoulder joint.

An analysis of error was performed for the calculation of mass moment of inertia for each body segment by the pendulum technique. The greatest contribution to error was the uncertainty in the measurements of segment length and distance from the segment center of mass to its fixed pendular axis. Assuming that each

of these distances could be measured to an accuracy of 2 mm, the estimated percent error in the value of the mass moment of inertia was 31, 20, 14, and 14% for phalangeal, carpometacarpal, antebrachial, and brachial segments, respectively. To our knowledge, only a single study⁵ in dogs has been published in which the mass moment of inertia for specific limb segments were measured,⁵ and in that study only the pelvic limb was evaluated. Additionally, the inertial data were used for calculation but were not directly reported, so that even gross comparison of values is not possible.

Limitations of our study include the 2-D analysis, the small number of dogs and trials in the experimental design (5 dogs with 3 trials each), and the inclusion of only mixed-breed dogs of a narrow weight range. Historically, 2-D studies of gait have justified this simplified approach by assuming that components of gait in the other planes are negligible. However, in a pathologically altered gait, treatment may be aimed at correcting anomalies that occur in the frontal and horizontal planes,³² and a complete gait analysis requires calculation of all variables in 3 dimensions. As our study was the first of its kind for the canine forelimb and intended to provide baseline values for further study, the motion out of the sagittal plane was considered negligible, and a 2-D design was used.

Dogs vary widely in size and proportion, perhaps even to a larger extent than the human population. Although the body segment parameter data in our study are probably representative of dogs 15 to 35 kg in body mass, it is unlikely to be broadly applicable to all dogs. However, the availability of published body segment parameter data for the thoracic limb will make complete dynamic gait analysis more feasible for use in clinically affected dogs. Dramatic, visually apparent differences in the overall conformation of the 6 mixed-breed dogs studied were not reflected in body segment parameter differences. Body segment parameters of the dogs in our study were strikingly similar, with SD of < 0.4% of body weight in mass, < 1 cm in length, and < 4% of segment length in location of center of mass. This suggests that the apparent conformational differences were based on familiar breed characteristics, such as ear and tail carriage, and other body segments, such as the head and torso. These differences, although visually dramatic and likely to affect measurement of other body segments, did not substantially affect those of the forelimb.

Ground reaction forces of our study are consistent with previously reported data. In a recent study,³⁷ 6 clinically normal large-breed dogs (25 to 38 kg) had a mean forelimb peak vertical force of $63.26 \pm 6.67\%$ of body weight at the walk, but craniocaudal force was not reported. In an earlier study,³⁸ ground reaction forces of the forelimbs and hind limbs were evaluated in 17 clinically normal dogs (8.6 to 58.5 kg) at a walk. The authors found a significant correlation between peak forelimb vertical force and body weight but only reported actual force values for a single representative trial. For that trial, peak vertical force was just under 70% of body weight, and peak craniocaudal force was approximately 12% of body weight. Results of our

study correlate well with these previously published values, with a mean peak vertical force of $62.60 \pm 4.53\%$ of body weight and a mean peak craniocaudal force of $11.55 \pm 2.31\%$ of body weight.

Any differences between the vertical intersegmental force at the joints (metacarpophalangeal, antebrachiocarpal, elbow, and shoulder in our study) and the ground reaction force indicate the effect of gravity and inertia at these joints. Because gravity does not affect craniocaudal forces, the differences in this direction are the result of inertial effects alone. Results of our study revealed only small differences between the ground reaction forces and the intersegmental forces at any joint during a walking gait, corresponding roughly to the findings of Bresler and Frankel² in the lower portion of the human limb.² The small overall difference is associated with small segment lengths, masses, mass moments of inertia of the canine forelimb, and the slow gait. A greater difference would be expected at faster gaits as the relative magnitude of the acceleration terms in the force and moment equations increases. To our knowledge, no veterinary studies have been published that report ground reaction forces and intersegmental forces together for any species at any gait, so that comparison is not possible. Although no substantial difference (on the basis of SD at each joint) in vertical intersegmental force was found between joints, a slight decrease in magnitude was found the more proximal the location of each joint.

Our kinematic data was consistent with the single published study³⁹ that examined forelimb kinematics in dogs at a walk. In that study, 3-D kinematic data were obtained from the forelimb and hind limb of 15 large-breed dogs (body mass; mean, 28.5 kg; range, 23.0 to 36.4 kg) throughout the entire gait cycle. Joint angular position was reported for several joints, including the elbow and carpal joints. During stance phase, the elbow joint had a pattern of flexion and extension similar to that observed in our study, with a mean maximum flexion angle of approximately 140°. The reported carpal joint angle required geometric conversion to match the angle convention adopted here. Once converted, it also had a pattern of flexion and extension similar to our findings, with an angle of approximately 190° for the first 3-quarters of stance followed by rapid extension at the end of stance. Those investigators did not examine the metacarpophalangeal joint.

In our study, a large extensor moment was calculated at the shoulder joint throughout stance, reflecting the role of the shoulder extensor muscles in support of the limb. The angular position and mechanical power of the shoulder were not calculated. To our knowledge, no forelimb gait analyses in quadrupeds have been published that report the moment or mechanical power at the shoulder joint. Results of the already described 3-D kinematic study³⁹ revealed flexion of the shoulder joint throughout most of stance from an initial flexion angle of approximately 140° to a minimum of approximately 120° with a shift toward extension just before lift-off in transition to the rapid flexion observed through the swing phase.

We calculated a large extensor moment at the elbow joint throughout much of the stance phase until

just before termination, when a smaller flexor moment was observed. This reflects the supportive role of the triceps muscle group at the elbow joint throughout stance. The power profile indicates negative work done against the extensor moment during the initial loading period, followed by a period of energy generation as the elbow extended through most of stance. In terminal stance, again a period of negative work corresponding with the shift toward a net flexor moment at take-off was observed. To our knowledge, no studies in dogs have evaluated net joint moments or mechanical power in the forelimb. In a study of the forelimb in horses at a walk,⁶ a large net extensor moment was calculated at the elbow joint during the first half of stance, followed by a large net flexor moment for the remainder of stance. The authors suggested that the flexor moment is seen from midstance during restrained extension of the elbow joint as the forelimb rotates over the stationary hoof in a manner analogous to the human hip joint. Mechanical power at the elbow joint was not calculated. In our study, a large flexor moment in the second half of stance was not observed, suggesting that the dynamics of the canine and equine elbow differ at the walking gait. It is possible that adaptation in the horse of the internal tendon of the biceps brachii muscle for passive support of the forelimb as part of the stay apparatus and for coordination of elbow joint flexion with shoulder joint flexion could be partly responsible for these differences.

In our study, a flexor moment was calculated at the antebrachioacarpal joint through most of the stance phase, despite continued extension of this joint through the first 3-quarters of stance. This is similar to the results reported⁸ for the carpus in horses at the walk, which was observed by those investigators to be similar to a phenomenon termed Lombard's paradox⁴⁰ that is commonly observed in the human knee joint.⁴¹ In humans, the hamstring muscles cross 2 joints and thus may produce simultaneous hip joint extensor and knee joint flexor moments while the knee joint is extending. In the study on horses,⁶ the authors did not suggest a mechanism for the phenomenon. In horses, activity by the flexors of the carpus through early stance at a walk has been shown by electromyographic analysis;⁴² however, to our knowledge, no electromyographic analysis of the functionally normal canine forelimb has been published for any gait. Such studies would be required to further investigate the contribution of the various muscles to the reported net joint moment. In our study, the power profile of the canine antebrachioacarpal joint revealed positive work by the extensors against the net flexor moment for the first 3-quarters of stance phase, followed by negative work in the final quarter of stance as a shift to an extensor moment was observed. This is in contrast to findings in horses⁶ where short periods of positive and negative work were done against the predominant flexor moment.

In our study, a flexor moment was calculated at the metacarpophalangeal joint through most of the stance phase while the angular position changed little. The mechanical power oscillated between positive and negative work but with a large SD, particularly in the latter half of stance. It is difficult to compare these values

to those of the metacarpophalangeal (fetlock) joint in the study in horses⁶ given the substantial variation in anatomy in the distal portion of the limb. One fundamental difference is that dogs walk with a digitigrade stance, whereas horses walk with an unguligrade stance, so that the conformation of the canine metacarpophalangeal joint is quite unlike that of the equine fetlock joint. Also, the equine distal forelimb flexor muscle-tendon units have specialized structure to form the passive stay apparatus, which is not found in dogs. The large magnitude and degree of variation in the power data reported for the metacarpophalangeal joint have 2 likely sources. When changes in angular position are small, they are amplified disproportionately during differentiation, and low amounts of noise in the data are more likely to affect results.³¹ Additionally, the segments that make up the joint are small in real and relative terms, so that even small errors in joint center position will have a greater effect on angular velocity and mechanical power values.

^aForce platform model 9865C, Kistler, Winterthur, Switzerland.

^bSun SparcStation 20, Sun Microsystems Inc, Mountain View, Calif.

^cApple Macintosh G3, Apple Computers, Cupertino, Calif.

^dCamera model HSC-180A, Motion Analysis Corp, Santa Rosa, Calif.

^eVideo image processor VP-320, Motion Analysis Corp, Santa Rosa, Calif.

^fReflective targets, Motion Analysis Corp, Santa Rosa, Calif.

^gBeuthanasia-D, Shering-Plough Co, Madison, NJ.

^hAdventurer AR3130 electronic balance, Ohaus, Pine Brook, NJ.

ⁱRVIT R60D, Shaevitz Sensors, Hampton, Va.

^jLabView, National Instruments, Austin, Tex.

^kMatLab, The Math Works Inc, Natick, Mass.

References

1. Winter DA. Mechanical power in human movement: generation, absorption, and transfer. *Med Sports Sci* 1987;25:34-45.
2. Bresler B, Frankel JP. The forces and moments in the leg during level walking. *Trans Am Soc Mech Eng* 1950;74:27-36.
3. DeCamp CE. Kinetic and kinematic gait analysis and the assessment of lameness in the dog. *Vet Clin North Am Small Anim Pract* 1997;27:825-840.
4. Clayton HM, Lanovaz JL, Schamhardt HC, et al. Net joint moments and powers in the equine forelimb during the stance phase of the trot. *Equine Vet J* 1998;30:384-389.
5. Dogan S, Manley PA, Vanderby RJ, et al. Canine intersegmental hip joint forces and moments before and after cemented total hip replacement. *J Biomech* 1991;24:397-407.
6. Colborne GR, Lanovaz JL, Spriggs EJ, et al. Forelimb joint moments and power during the walking stance phase of horses. *Am J Vet Res* 1998;59:609-614.
7. Clayton HM, Hoyt DF, Wickler SJ, et al. Hindlimb net joint energies during swing phase as a function of trotting velocity. *Equine Vet J Suppl* 2002;34:363-6.
8. Clayton HM, Hodson E, Lanovaz JL, et al. The hindlimb in walking horses: 2. Net moments and joint powers. *Equine Vet J* 2001;33:44-8.
9. Harless E. Die statischen Momente der menschlichen Gliedmassen. *Abhandl Mathematische-Physikalischen Classe Konigl Sachsichen Ges Wissenschaft* 1860;8:69-96.
10. Braune W, Fischer O. Determination of the moments of inertia of the human body and its limbs. In: Cappozzo A, Marchetti M, Tosi V, eds. *Biomechanics: a century of research using moving pictures*. 26th ed. Rome: Promograph, 1988;125.
11. Fischer O. *Theoretische Grundlagen für eine Mechanik der lebenden Körper mit speziellen Anwendungen auf den Menschen, sowie auf einige Bewegungs-Vorgänge an Maschinen*. Berlin: BG Teubner, 1906 (ATI 153668, Available from Defense Documentation Center)
12. Dempster WT. Space requirements of the seated operator.

WADC Technical Report (TR-55-159);Ohio: Wright-Patterson Air Force Base, 1955.

13. Clauser CE, McConville JT, Young JW. Weight, volume, and center of mass of segments of the human body. *AMRL Technical Report (TR-69-70)*;Ohio: Wright-Patterson Air Force Base, 1969.

14. Chandler RF, Clause CE, McConville JT, et al. Investigation of inertial properties of the human body. *AMRL Technical Report (TR-74-137)*; City, Ohio: Wright Patterson Air Force Base, 1975.

15. Mori M, Yamanoto T. Die Massenanteile der einzelnen Körperabschnitte der Japaner. *Acta Anat* 1959;37:385–388.

16. Fujikawa K. The center of gravity in the parts of the human body. *Okajimas Folia Anat Jpn* 1963;39:117–125.

17. Liu YK, Laborde JM, Van Buskirk WC. Inertial properties of a segmented cadaver trunk: their implications in acceleration injuries. *Aerospace Med* 1971;42:650–657.

18. Miller DI, Nelson RC. *The biomechanics of sport; a research approach*. Philadelphia: Lea & Febiger, 1973;39–87

19. Little MJ, Jessup GT. Determining limb volume by a point gauge, water-displacement technique. *Res Q Exerc Sport* 1977;48: 239–243.

20. Kaleps I, Clauser CE, Young JW, et al. Investigation into the mass distribution properties of the human body and its segments. *Ergonomics* 1984;27:1225–1237.

21. Deter RL, Harrist RB, Hadlock FP, et al. Longitudinal studies of fetal growth using volume parameters determined with ultrasound. *J Clin Ultrasound* 1984;12:313–324.

22. Labs KH, Tschoepel M, Gamba G, et al. The reliability of leg circumference assessment: a comparison of spring tape measurements and optoelectronic volumetry. *Vasc Med* 2000;5:69–74.

23. Stanton AW, Northfield JW, Holroyd B, et al. Validation of an optoelectronic limb volumeter (Perometer). *Lymphology* 1997;30:77–97.

24. Elia M, Fuller NJ, Hardingham CR, et al. Modeling leg sections by bioelectrical impedance analysis, dual x-ray absorptiometry, and anthropometry: assessing segmental muscle volume using magnetic resonance imaging as a reference. *Ann N Y Acad Sci* 2000;904:298–305.

25. Kamber M, Koster M, Kries R, et al. Creatine supplementation—Part I: performance, clinical chemistry, and muscle volume. *Med Sci Sports Exerc* 1999;31:1763–1769.

26. Berg HE, Tedner B, Tesch PA. Changes in lower limb muscle cross-sectional area and tissue fluid volume, after transition from standing to supine. *Acta Physiol Scand* 1993;148:379–385.

27. Buckley DC, Kudsk KA, Rose BS, et al. Anthropometric and

computerized tomographic measurements of lower extremity lean body mass. *J Am Diet Assoc* 1987;87:196–199.

28. Maughan RJ, Abel RW, Watson JS, et al. Forearm composition in trained and untrained limbs. *Clin Physiol* 1986;6:389–396.

29. Overend TJ, Cunningham DA, Paterson DH, et al. Computed tomographic assessment of the thigh in young and old men. *Can J Appl Physiol* 1993;18:263–273.

30. McLaughlin RJ Jr, Roush JK. Effects of subject stance time and velocity on ground reaction forces in clinically normal Greyhounds at the trot. *Am J Vet Res* 1994;55:1666–1671.

31. Winter DA. *Biomechanics and motor control of human movement*. 2nd ed. New York: John Wiley & Sons, 1990;51–102.

32. Apkarian J, Naumann S, Cairns B. A three-dimensional kinematic and dynamic model of the lower limb. *J Biomech* 1989; 22:143–155.

33. Schaefer SL, DeCamp CE, Hauptman JG, et al. Kinematic gait analysis of hind limb symmetry in dogs at the trot. *Am J Vet Res* 1998;59:680–685.

34. van Weeren PR, van den Bogert AJ, Barneveld A. Quantification of skin displacement near the carpal, tarsal, and fetlock joints of the walking horse. *Equine Vet J* 1988;20:203–208.

35. van Weeren PR, van den Bogert AJ, Barneveld A. Quantification of skin displacement in the proximal parts of the limbs of the walking horse. *Equine Vet J* 1990;suppl 9:110–118.

36. van den Bogert AJ, van Weeren PR, Schamhardt HC. Correction for skin displacement errors in movement analysis of the horse. *J Biomech* 1990;23:97–101.

37. Conzemius MG, Aper RL, Hill CM. Evaluation of a canine total-elbow arthroplasty system: a preliminary study in normal dogs. *Vet Surg* 2001;30:11–20.

38. Budsberg SC, Verstraete MC, Soutas-Little RW. Force plate analysis of the walking gait in healthy dogs. *Am J Vet Res* 1987; 48:915–918.

39. Hottinger HA, DeCamp CE, Olivier NB, et al. Noninvasive kinematic analysis of the walk in healthy large-breed dogs. *Am J Vet Res* 1996;57:381–388.

40. Lombard WP. The action of two-joint muscles. *Am Phys Educ Rev* 1903;8:141–145.

41. Andrews JG. The functional roles of the hamstrings and quadriceps during cycling: Lombard's Paradox revisited. *J Biomech* 1987;20:565–575.

42. Jansen MO, van Raaij JA, van den Bogert AJ, et al. Quantitative analysis of computer-averaged electromyographic profiles of intrinsic limb muscles in ponies at the walk. *Am J Vet Res* 1992;53:2343–2349.